Electronic Supplementary Material (ESI) for Physical Chemistry Chemical Physics.


# Supporting Information

# Light-driven reduction of $CO_2$: thermodynamics and kinetics of hydride transfer reactions in benzimidazoline derivatives

B. D. Ostojić[1], B. Stanković[2], and D. S. Đorđević[1] and P. Schwerdtfeger[3]

[1]*Center of Excellence in Environmental Chemistry and Engineering, Institute for Chemistry, Technology and Metallurgy, University of Belgrade, Njegoševa 12, Belgrade 11158, Serbia*

[2]*Faculty of Physical Chemistry, University of Belgrade, Studentski trg 12-16, 11000 Belgrade, Serbia*

[3] *Centre for Theoretical Chemistry and Physics (CTCP), The New Zealand Institute for Advanced Study (NZIAS), Massey University Auckland, Private Bag 102904, North Shore City, 0745 Auckland, New Zealand*

## Contents



## 1. Computational Methods

In order to analyze in detail the energy differences between the ground and the first excited electronic state of the **1a**···$CO_2$ complex along the hydride transfer reaction coordinate for dimethylsulfoxide (DMSO) as a solvent, the APFD,[1] ωB97XD,[2] and TPSSh[3,4] functionals were applied in addition to the ones already discussed in the main text. The cLR-PCM continuum model corrected for linear response solvation (cLR) scheme for solvent effects[5] on the excited state was used[6,7,8,9,10] as implemented in Gaussian16.[11] The energies of the ground and first three excited states were also obtained with the complete-active-space self-consistent-field (CASSCF)[12,13] method complemented by second-order multireference perturbation theory (CASPT2) using the internally contracted multi-reference second-order perturbation theory code (RS2C)[14] as implemented in Molpro.[15] Four doubly occupied π orbitals, one doubly occupied σ orbital and five lowest unoccupied orbitals have been selected for the active space (Figure S1) in the state-averaged CASSCF calculations performed, including four singlet states with equal weights. Molecular orbitals of the ground and first excited state of the **1a**···$CO_2$ complex and the ground state of the **2a**···$HCO_2^-$ complex at the corresponding equilibrium geometries involved in the electronic states are shown in Figures S2 for the CASSCF/CASPT2 calculations and S3 for the DFT calculations.

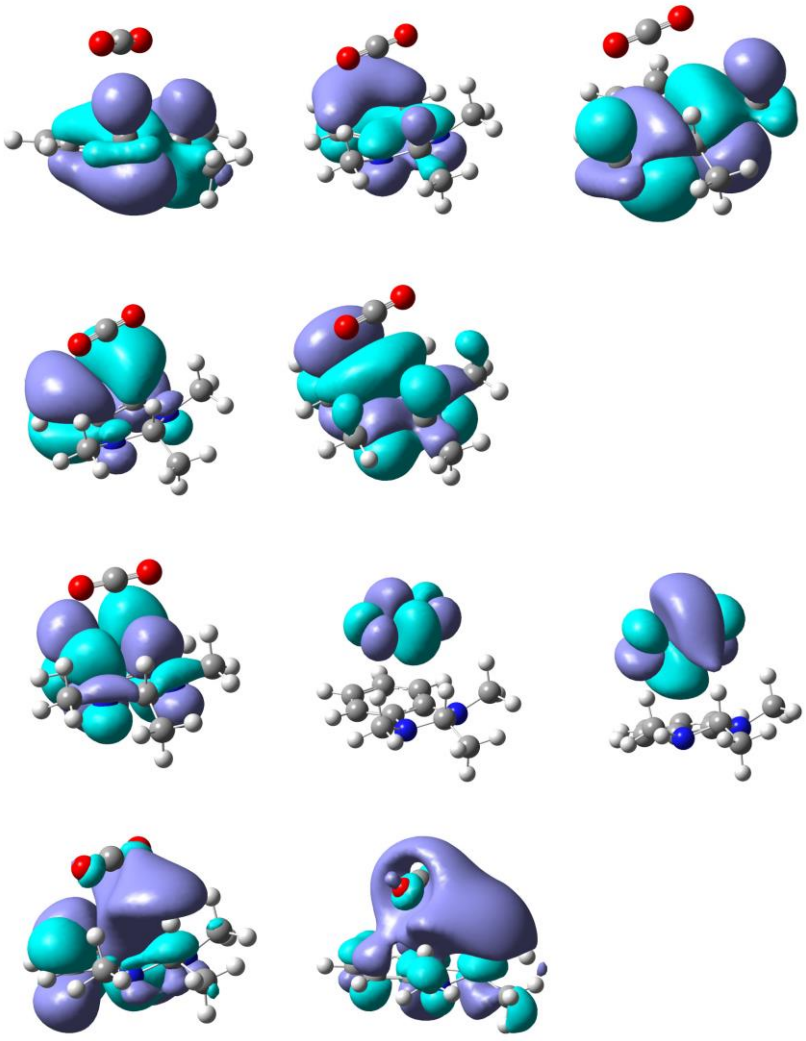

**Figure S1. Molecular orbitals included in the active space of the CASSCF/CASPT2 calculations obtained at the optimized geometry of the ground state of the 1a•••$CO_2$ complex.**

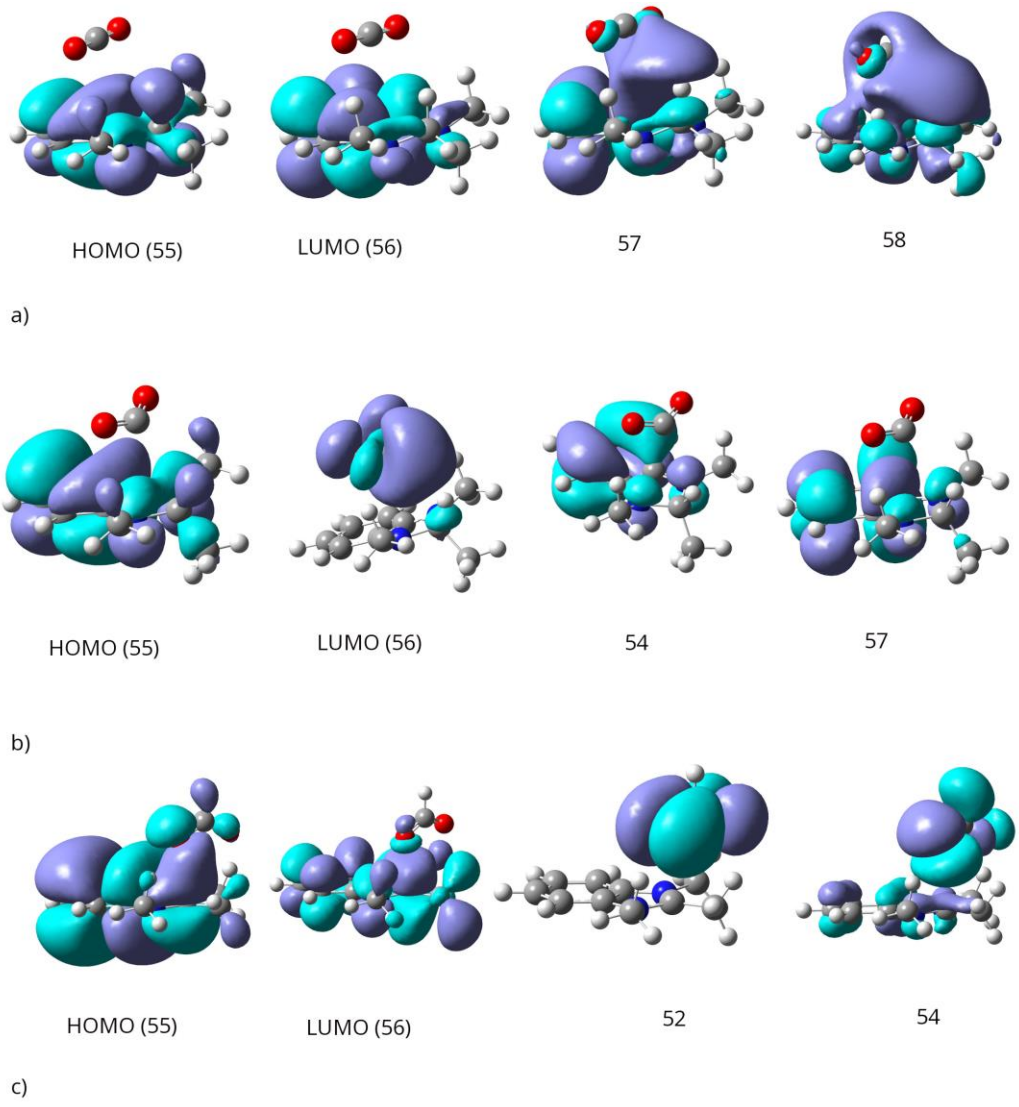


**Figure S2. Important natural orbitals from the CASSCF calculations obtained at the equilibrium geometry of the 1a•••$CO_2$ complex in its ground state (panel a), in its first excited state (panel b), and at the equilibrium geometry of the ground state of the 2a•••$HCO_2^-$ complex (panel c).**

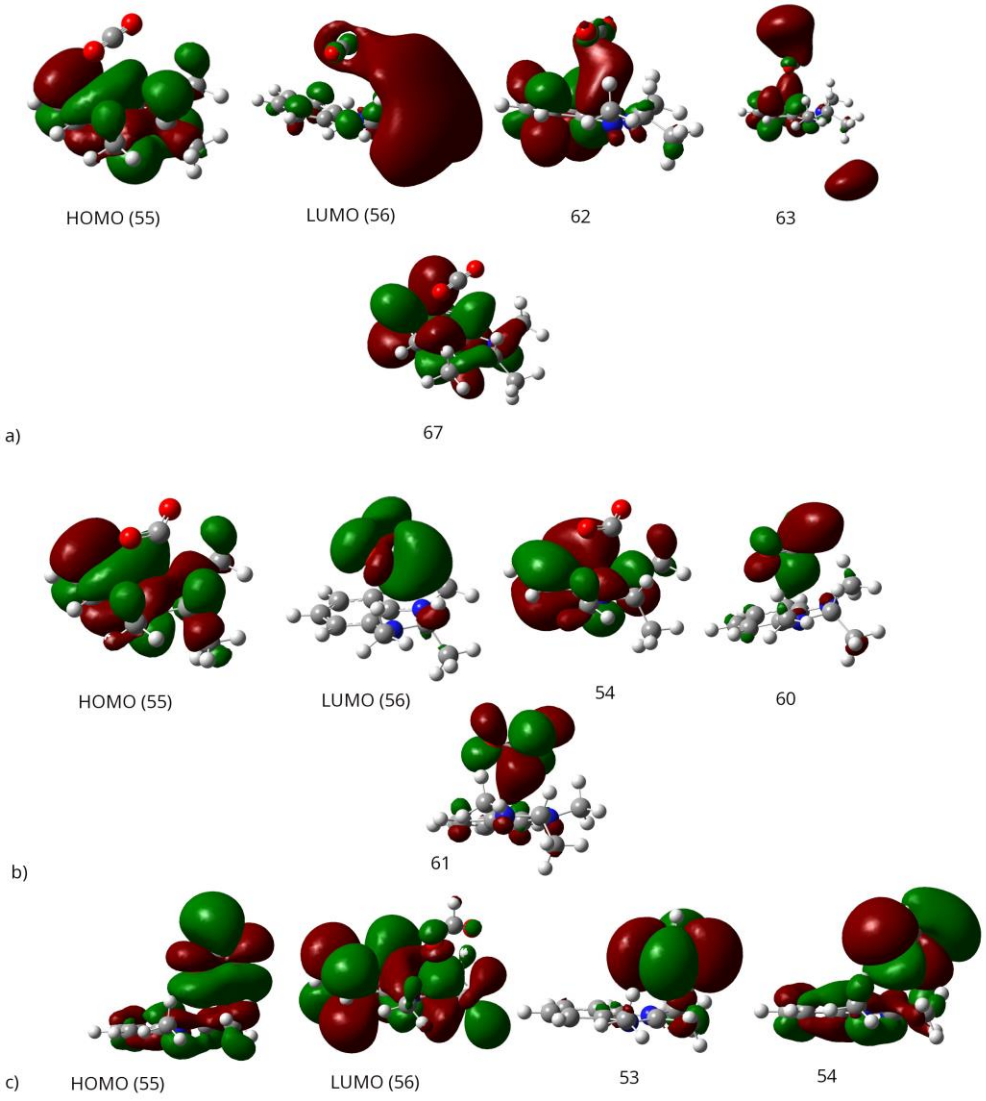


**Figure S3 Important molecular orbitals from the DFT (ωB97XD) calculations obtained at the equilibrium geometry of the 1a•••$CO_2$ complex in its ground state (panel a), in its first excited state (panel b), and at the equilibrium geometry of the ground state of the 2a•••$HCO_2^-$ complex (panel c).**

## 3. Hydride transfer profiles in the 1a···$CO_2$ complex

Figures S4, S5 and S6 show hydride transfer reaction pathways with DMSO as the solvent obtained from single-point calculations at the (TD)-APFD/aug-cc-pVDZ, (TD)-ωB97XD/aug-cc-pVDZ and (TD)-TPSSh/aug-cc-pVDZ levels of theory, respectively, along the reaction coordinate for the first excited state of the **1a**···CO2 complex. In going from **1a** + $CO_2$ to **2a** + $HCOO^-$, the IRC pathway is the same as in Figure 11 of the main text of the manuscript. Notice that the energy profiles displayed in Figs. S4, S5 and S6 are qualitatively similar to the profile given in Figure 11. At an energy of ~2 eV and reaction coordinate of ~-8, the PES of the first excited state either crosses or lies energetically close to the ground state of the **1a**···$CO_2$ complex.

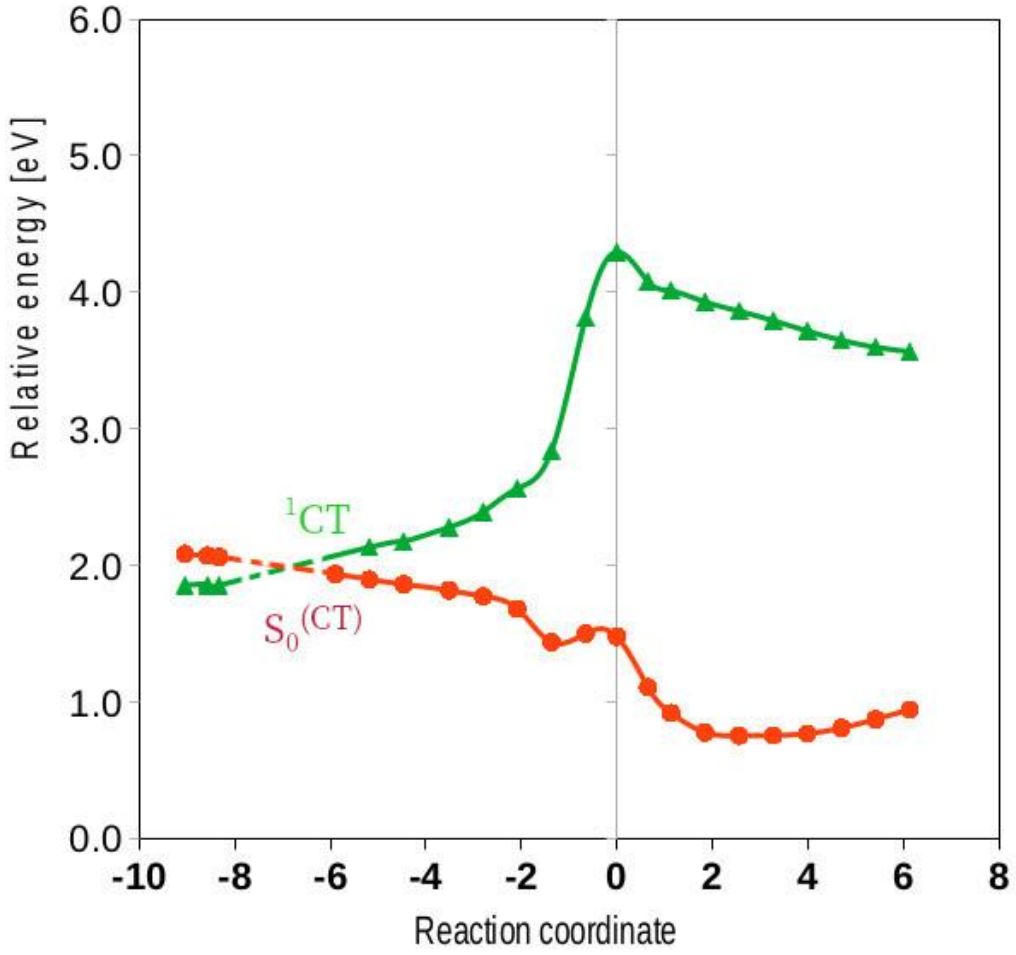


**Figure S4. Hydride transfer profile in the 1a···$CO_2$ complex obtained as single-point calculations at the (TD)-APFD/aug-cc-pVDZ level of theory on top of excited state IRC obtained at the TD-ωB97X-D/6-31+G(d,p) level of theory with DMSO as the solvent. The reaction coordinate is defined in mass weighted coordinates (Bohr ($AMU^{-1/2}$). Dashed lines indicate diabatic correlation of the states.**

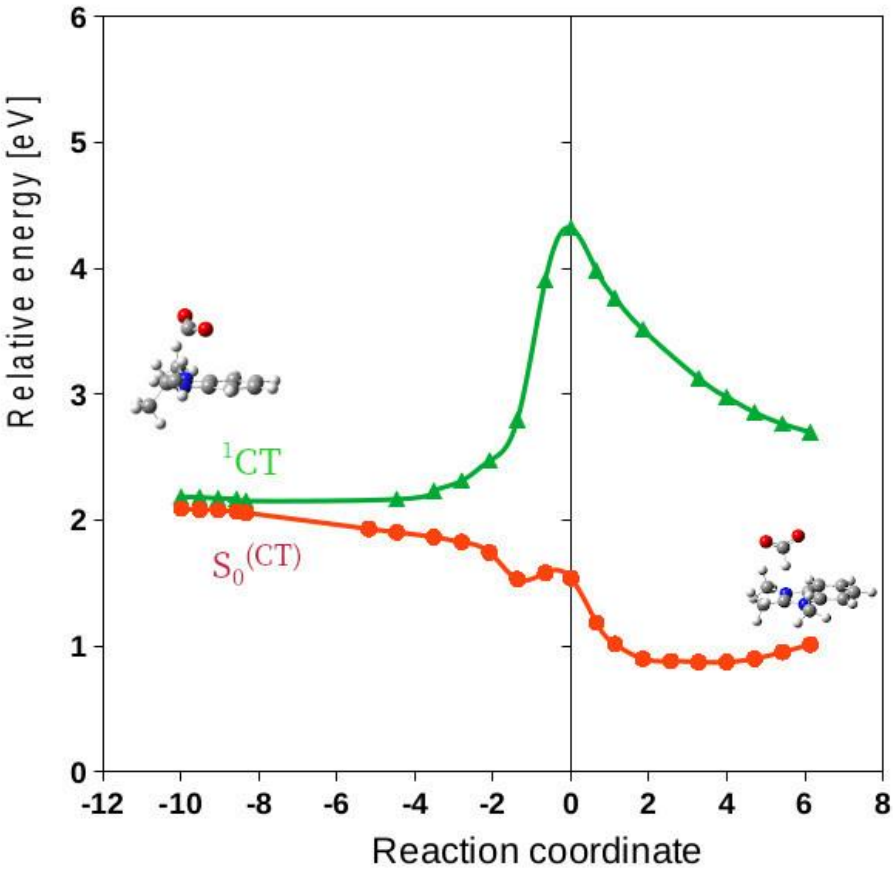


**Figure S5. Hydride transfer profile in the 1a···$CO_2$ complex obtained as single-point calculations at the (TD)-ωB97X-D/aug-cc-pVDZ level of theory on top of excited state IRC obtained at the TD-ωB97X-D/6-31+G(d,p) level of theory with DMSO as the solvent. The reaction coordinate is defined in mass weighted coordinates (Bohr ($AMU^{-1/2}$)).**

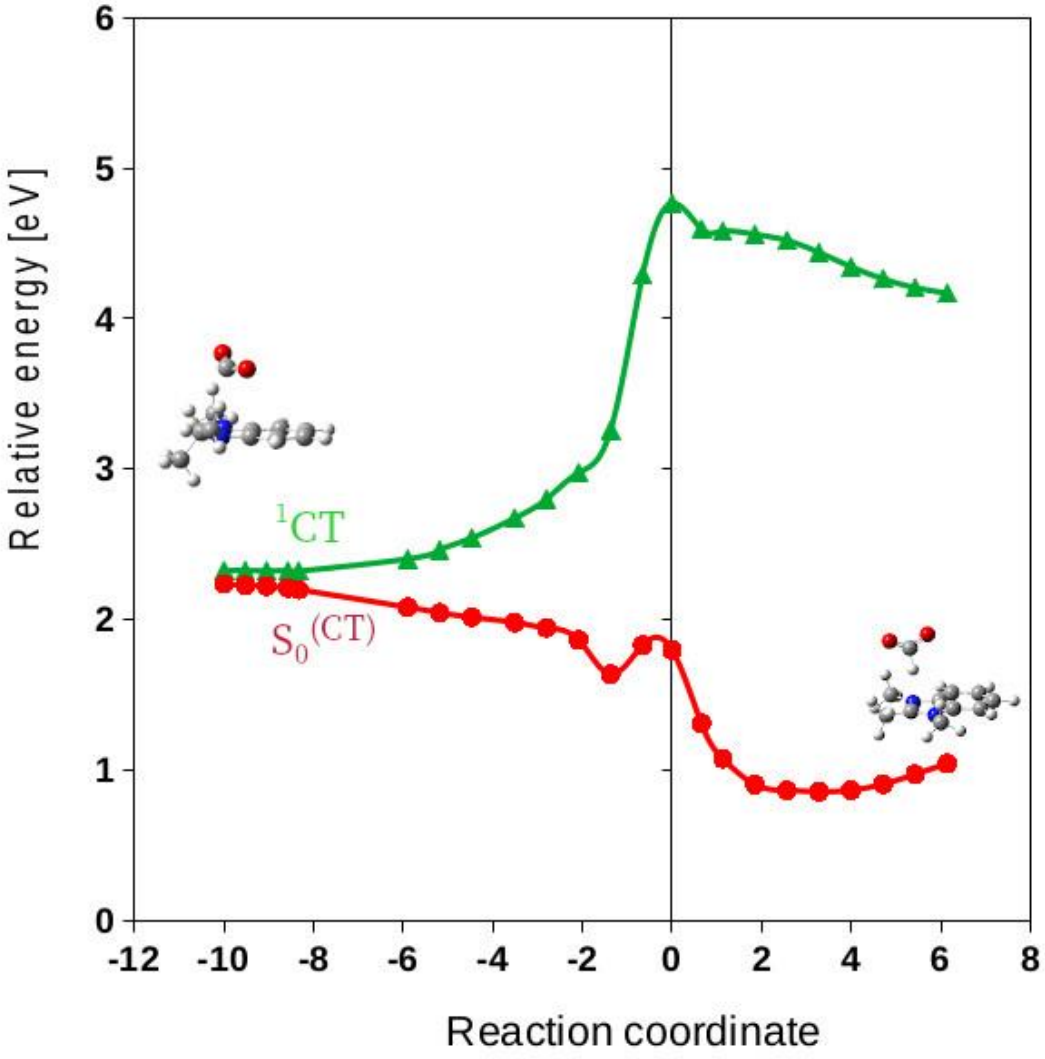


**Figure S6. Hydride transfer profile in the 1a···$CO_2$ complex obtained as single-point calculations at the (TD)-TPSSh/aug-cc-pVDZ level of theory on top of excited state IRC obtained at the TD-ωB97X-D/6-31+G(d,p) level of theory with DMSO as the solvent. The reaction coordinate is defined in mass weighted coordinates (Bohr ($AMU^{-1/2}$)).**

## 4. The IRC reaction coordinate and critical C-H bonds and O-C-O angles

The reaction coordinate for the hydride transfer reaction in the excited state mainly involves changing the distance between the carbon of $CO_2$ and the hydrogen of the organo-hydride coupled with the out-of-plane distortion of the five-membered ring system of the benzimidazoline unit, and rotation/movement of the corresponding methyl groups. In addition to the abovementioned changes, the reaction coordinate for the hydride transfer reaction in the ground state involves also the changes in the O-C-O bending angle. The critical values of the C-H bond of the benzimidazoline derivative **1a** and the O-C-O angle along the intrinsic reaction coordinate pathway for the hydride transfer in the ground and excited electronic states are presented in Table S1. The minus sign for the reaction coordinate implies reverse direction, while plus sign for the reaction coordinate means forward direction.

**Table S1**

| ground state | | | first singlet excited state | | |
|---|---|---|---|---|---|
| $r_c$ | C-H [Å] | O-C-O [º] | $r_c$ | C-H [Å] | O-C-O [º] |
| -10.3 | 1.112 | 179.3 | -12.0 | 1.091 | 136.1 |
| -9.0 | 1.111 | 179.2 | -11.0 | 1.091 | 136.2 |
| -8.0 | 1.109 | 179.2 | -10.0 | 1.091 | 136.3 |
| -7.0 | 1.108 | 179.1 | -9.0 | 1.092 | 136.4 |
| -6.0 | 1.106 | 179.1 | -8.0 | 1.090 | 136.6 |
| -5.0 | 1.102 | 179.2 | -7.0 | 1.088 | 137.1 |
| -4.0 | 1.098 | 179.1 | -6.0 | 1.085 | 137.9 |
| -3.0 | 1.093 | 178.6 | -5.0 | 1.083 | 138.6 |
| -2.0 | 1.092 | 173.3 | -4.0 | 1.081 | 139.3 |
| -1.0 | 1.120 | 159.2 | -3.0 | 1.078 | 140.4 |
| 0.0 | 1.313 | 145.1 | -2.0 | 1.073 | 142.3 |
| 1.0 | 1.624 | 136.5 | -1.0 | 1.117 | 143.2 |
| 2.0 | 1.756 | 132.9 | 0.0 | 1.590 | 139.7 |
| 3.0 | 1.878 | 131.4 | 1.0 | 1.972 | 136.6 |
| 4.0 | 1.973 | 130.7 | 2.0 | 2.026 | 138.1 |
| 5.0 | 2.045 | 130.2 | 3.0 | 2.635 | 139.7 |
| 6.0 | 2.118 | 129.9 | 4.0 | 2.954 | 140.2 |
| 7.0 | 2.187 | 129.7 | 5.0 | 3.248 | 140.6 |
| 8.0 | 2.248 | 129.6 | 6.0 | 3.508 | 141.6 |
| 9.0 | 2.327 | 129.4 | 7.0 | 3.707 | 142.7 |
| 10.0 | 2.459 | 129.2 | 8.0 | 3.840 | 143.7 |
| 11.0 | 2.642 | 129.0 | 9.0 | 3.933 | 144.6 |
| 12.0 | 2.861 | 128.9 | 10.0 | 3.990 | 145.3 |
| 12.2 | 2.896 | 128.8 | 11.0 | 4.034 | 145.9 |
| | | | 11.9 | 4.070 | 146.2 |

**Table S2. Calculated partial atomic charges (NPA) at the CAM-B3LYP/6-311+G(2d,p) level of theory for the transferred hydride at the optimized TS geometry in the ground electronic state of the 1a···$CO_2$ and 1d···$CO_2$ complexes and 1a and 1d species for the gas phase and DMSO.**

| | $q(H)_{TS}$ (1a···$CO_2$) | $q(H)_{donor}$ (1a) | $q(H)_{TS}$ (1d···$CO_2$) | $q(H)_{donor}$ (1d) |
|---|---|---|---|---|
| **gas phase** | **0.020** | **0.150** | **0.022** | **0.150** |
| **DMSO** | **0.016** | **0.167** | **0.017** | **0.167** |

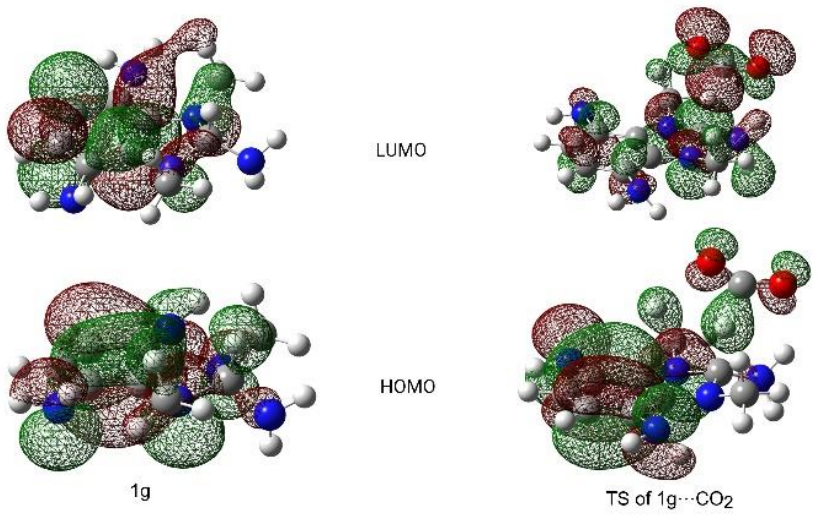


**Figure S7. HOMO and LUMO of 1g (right) and the corresponding transition state (TS) (left) for the HT reaction in the 1g···$CO_2$ complex.**

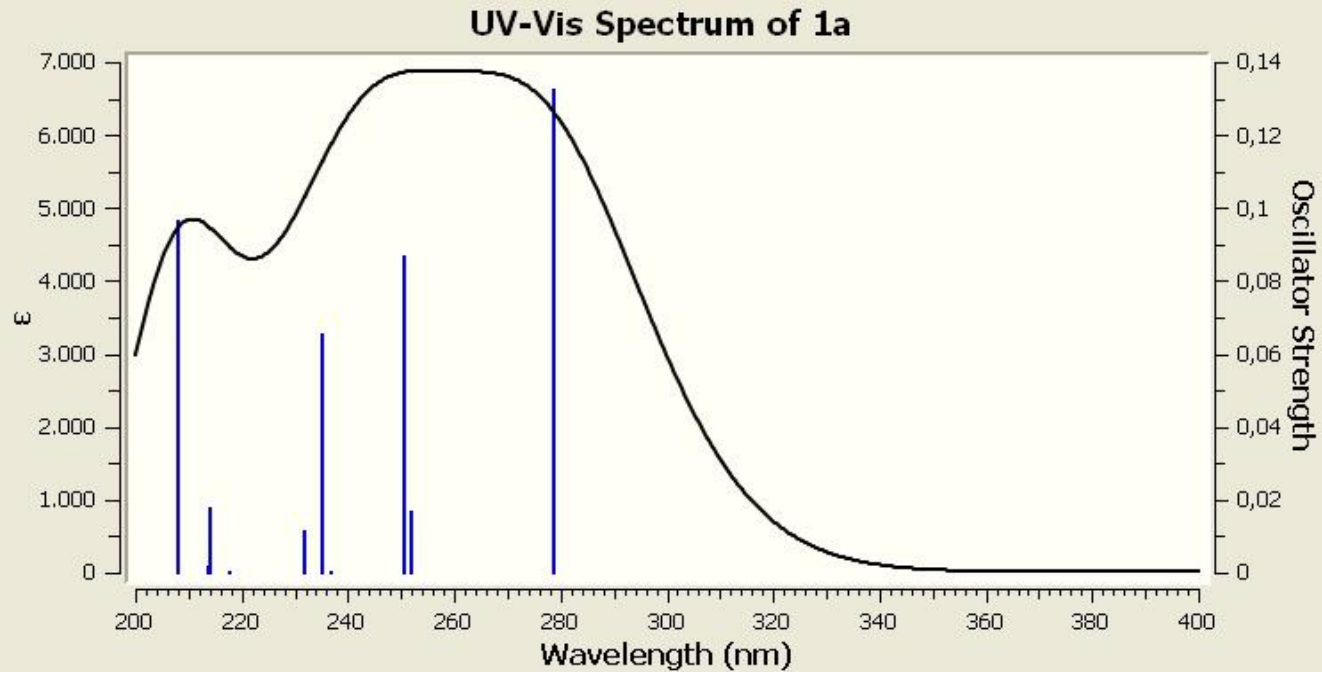


**Figure S8. UV-vis spectrum of gas phase of 1a at the ωB97XD/aug-cc-pVDZ level of theory.**

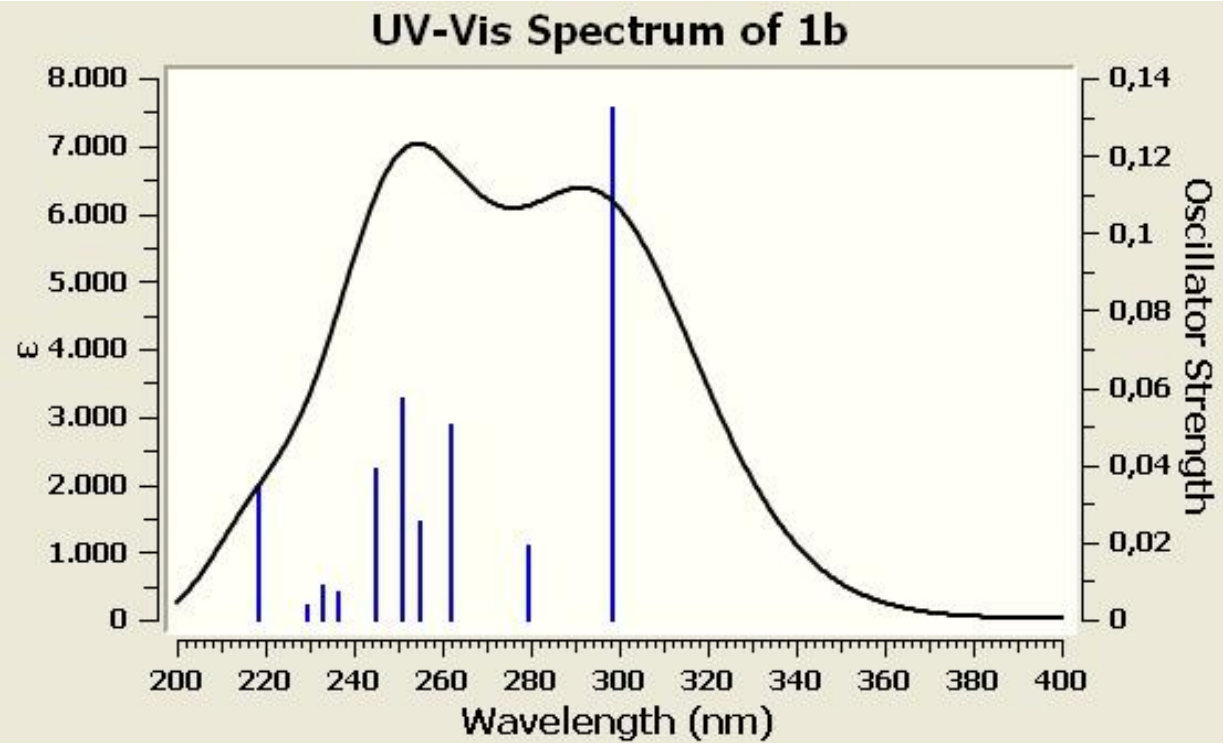


**Figure S9. UV-vis spectrum of gas phase of 1b at the ωB97XD/aug-cc-pVDZ level of theory.**

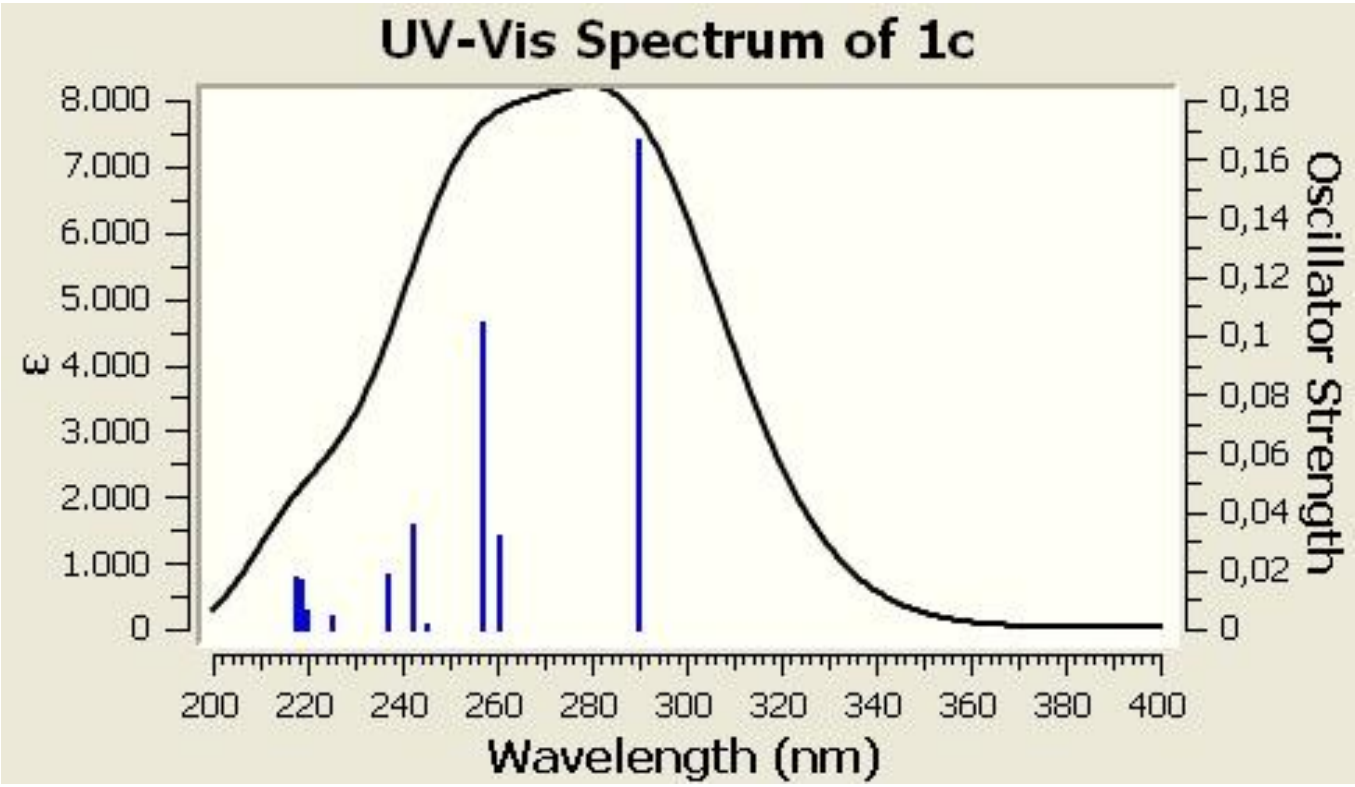


**Figure S10. UV-vis spectrum of gas phase of 1c at the ωB97XD/aug-cc-pVDZ level of theory.**

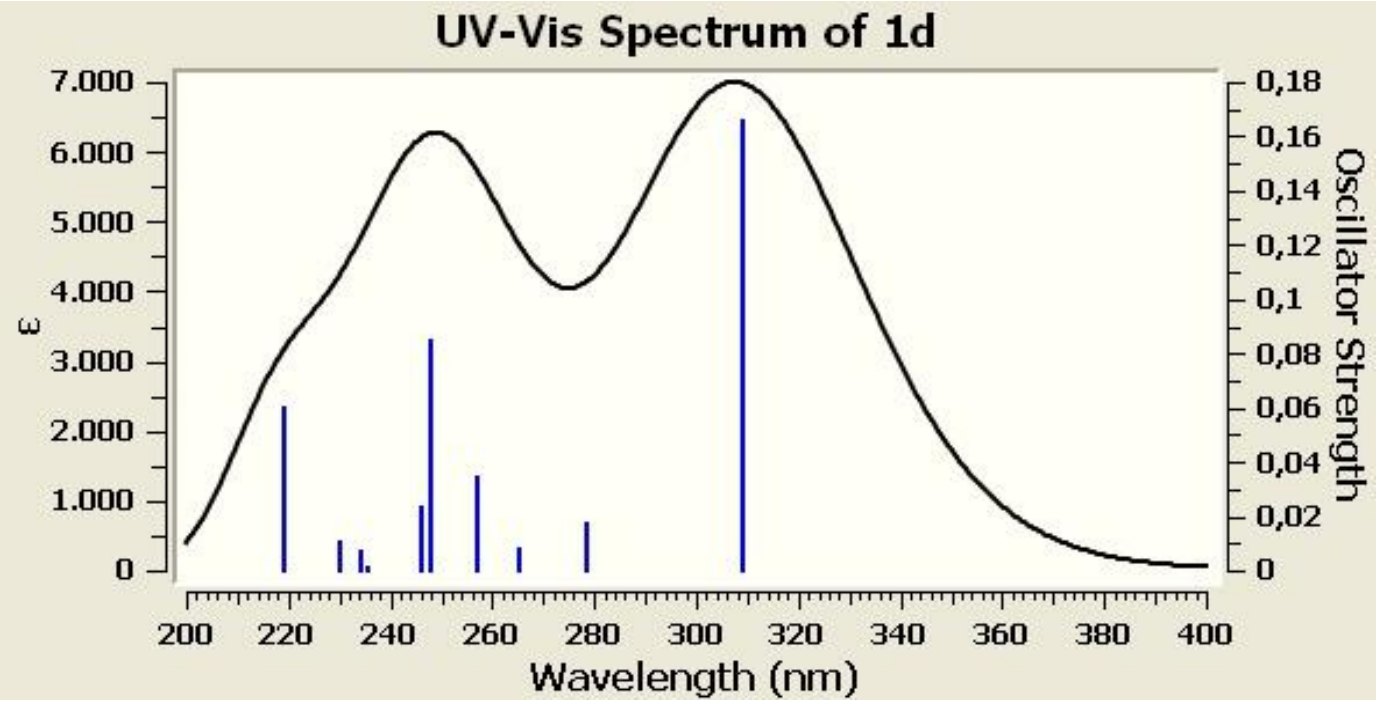


**Figure S11. UV-vis spectrum of gas phase of 1d at the ωB97XD/aug-cc-pVDZ level of theory.**

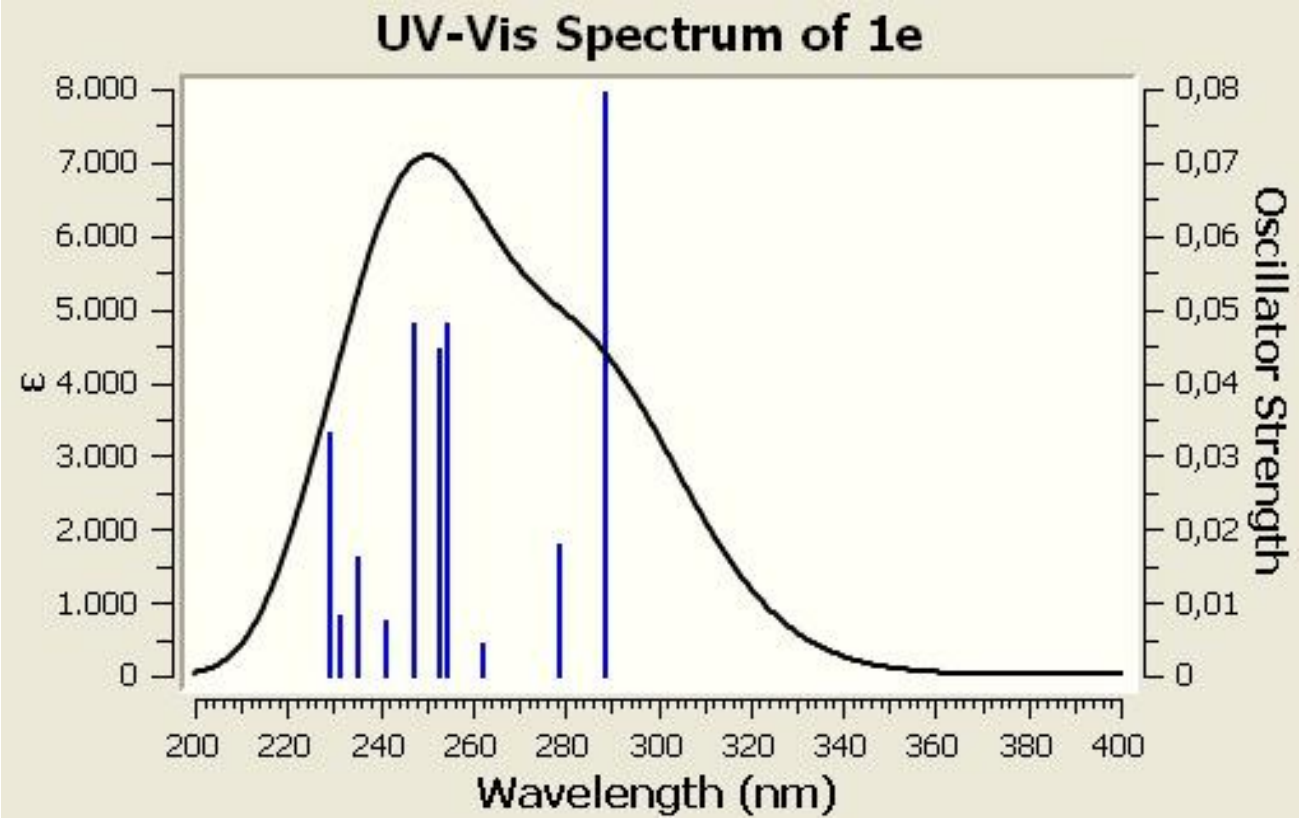


**Figure S12. UV-vis spectrum of gas phase of 1e at the ωB97XD/aug-cc-pVDZ level of theory.**

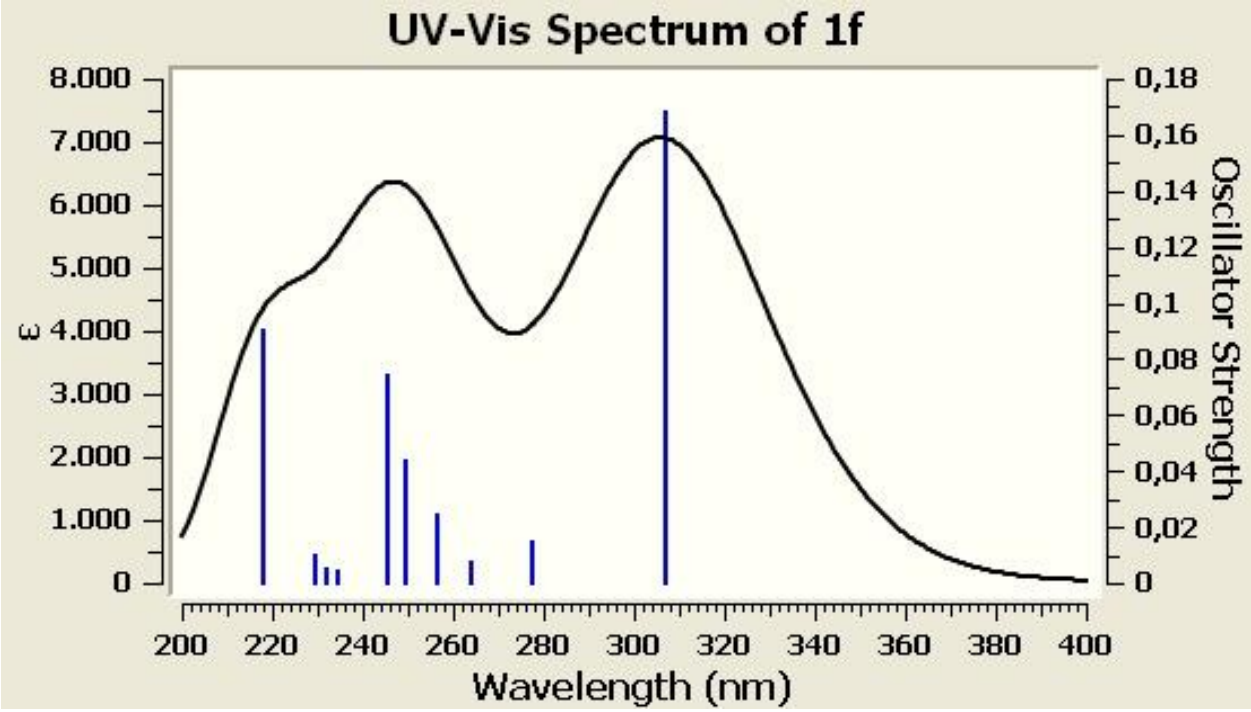


**Figure S13. UV-vis spectrum of gas phase of 1f at the ωB97XD/aug-cc-pVDZ level of theory.**

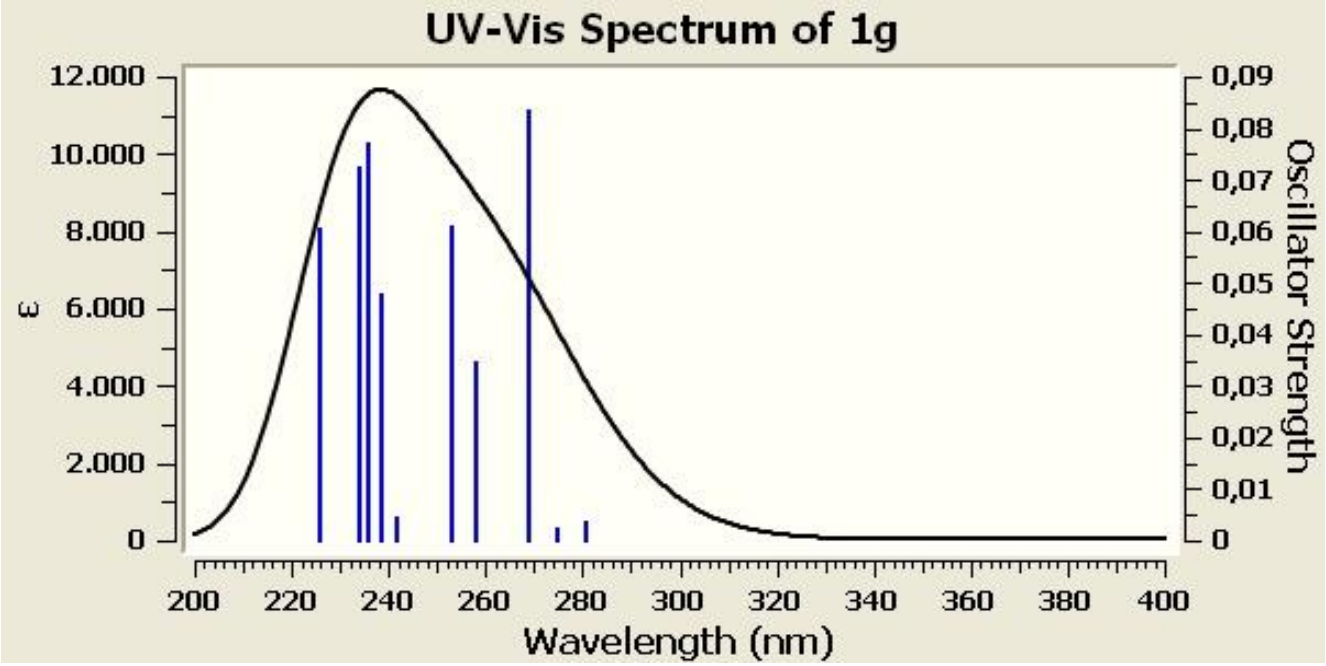


**Figure S14. UV-vis spectrum of gas phase of 1g at the ωB97XD/aug-cc-pVDZ level of theory.**

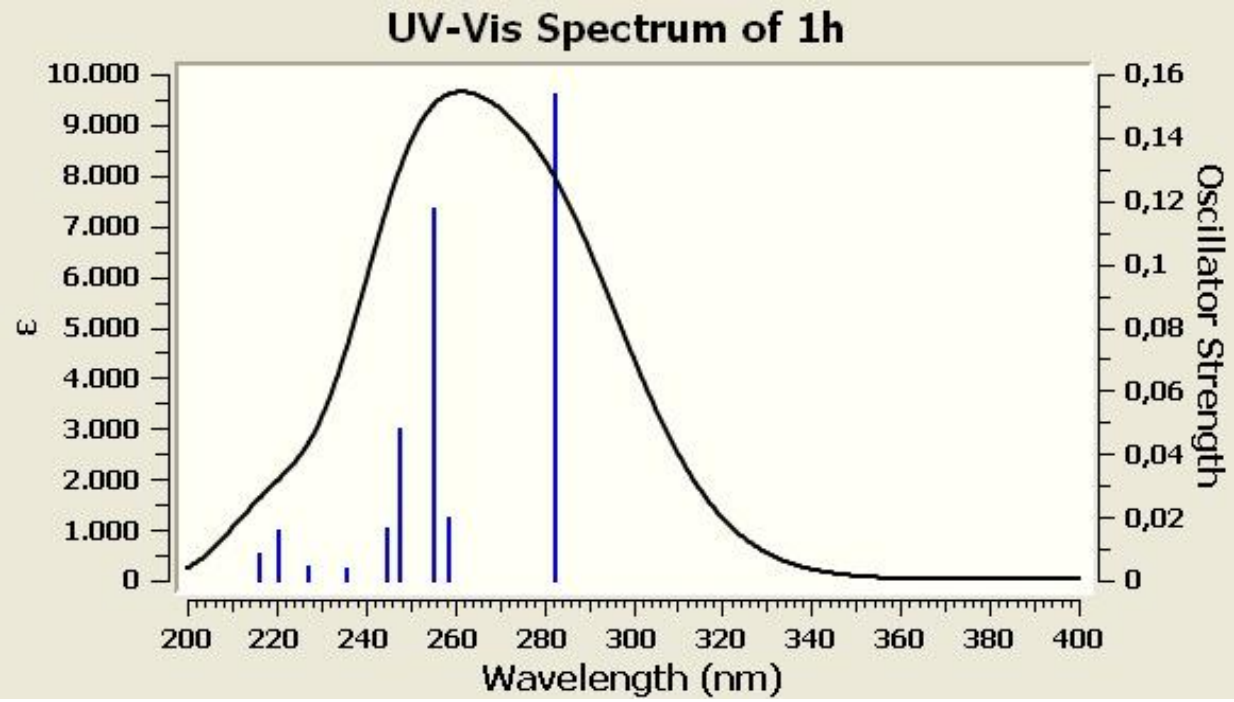


**Figure S15. UV-vis spectrum of gas phase of 1h at the ωB97XD/aug-cc-pVDZ level of theory.**

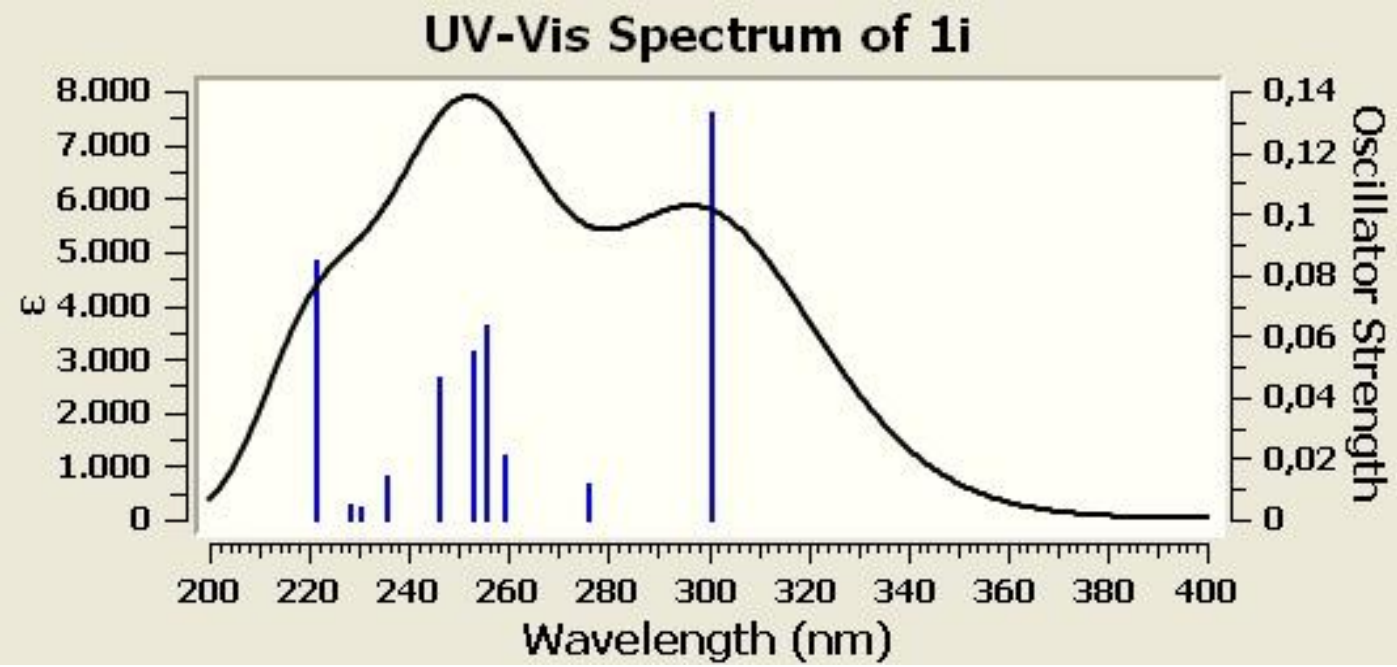


**Figure S16. UV-vis spectrum of gas phase of 1i at the ωB97XD/aug-cc-pVDZ level of theory.**

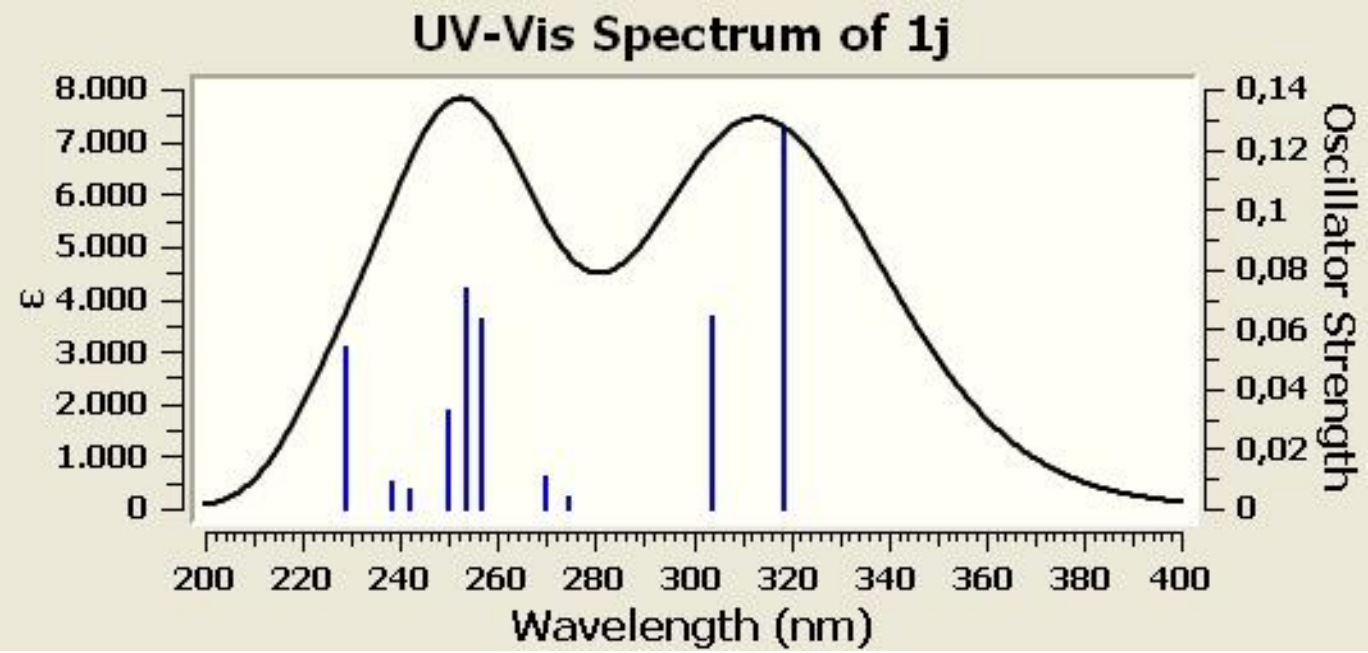


**Figure S17. UV-vis spectrum of gas phase of 1j at the ωB97XD/aug-cc-pVDZ level of theory.**

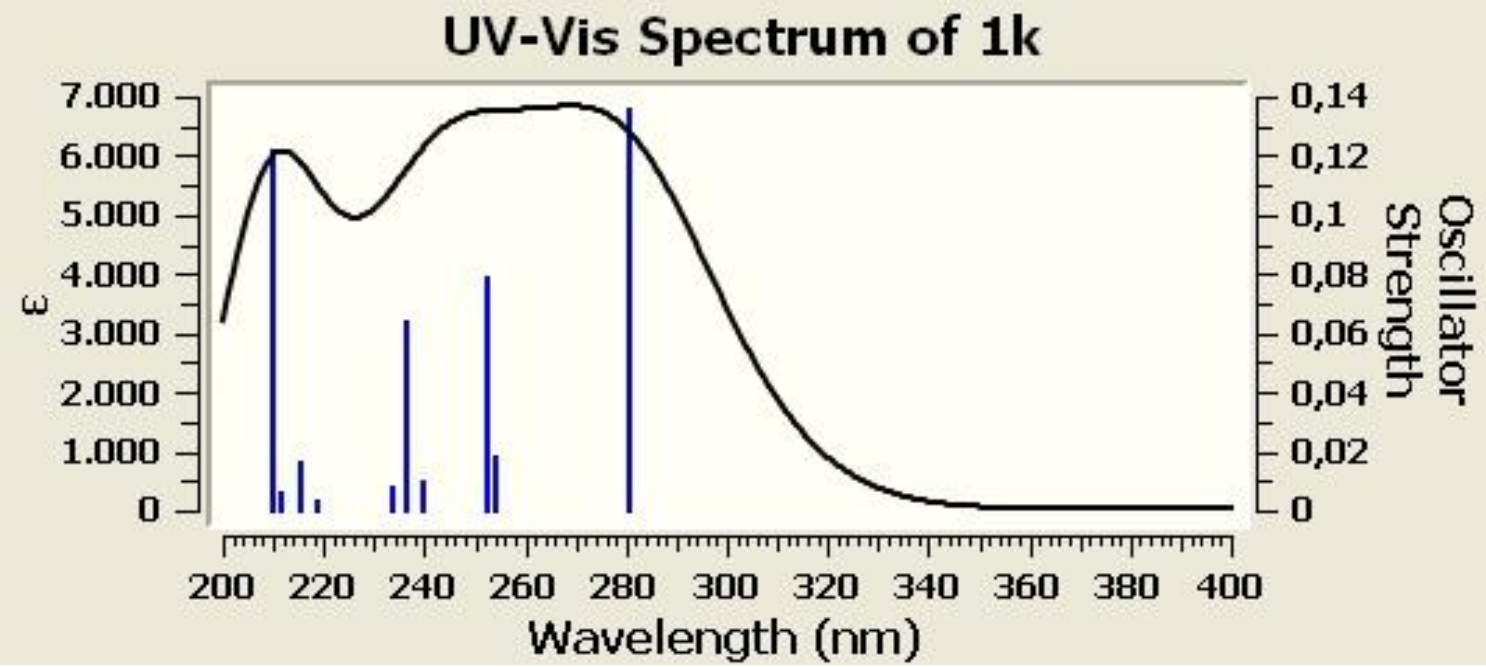


**Figure S18. UV-vis spectrum of gas phase of 1k at the ωB97XD/aug-cc-pVDZ level of theory.**

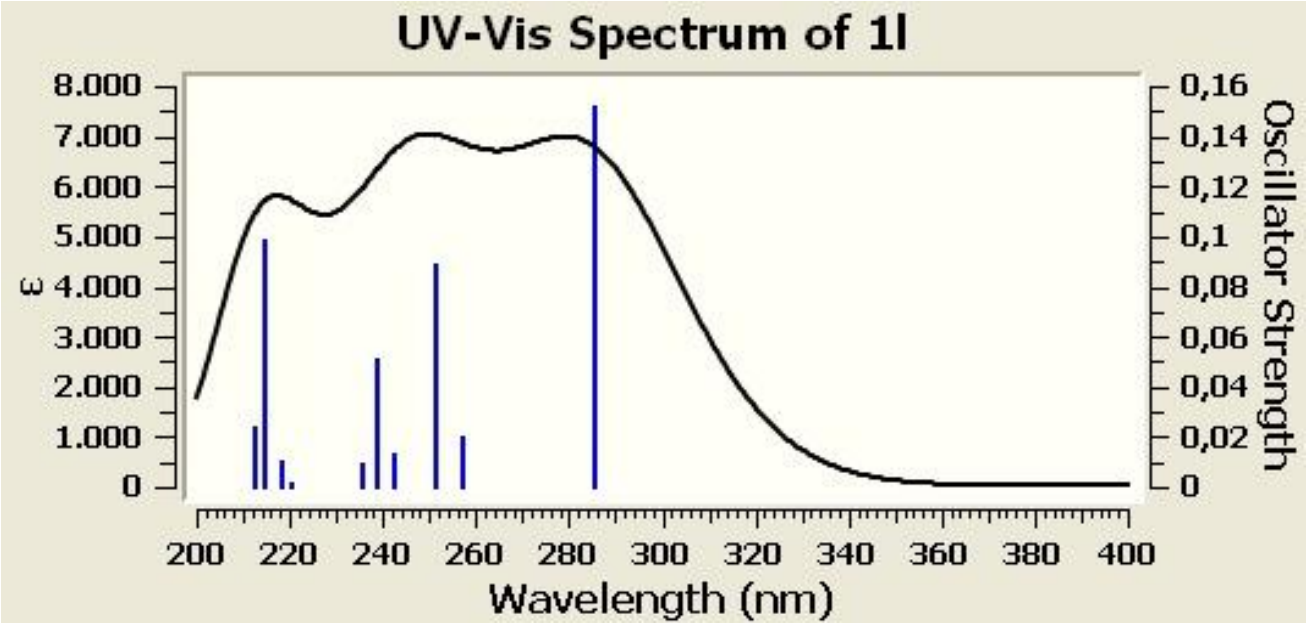


**Figure S19. UV-vis spectrum of gas phase of 1l at the ωB97XD/aug-cc-pVDZ level of theory.**

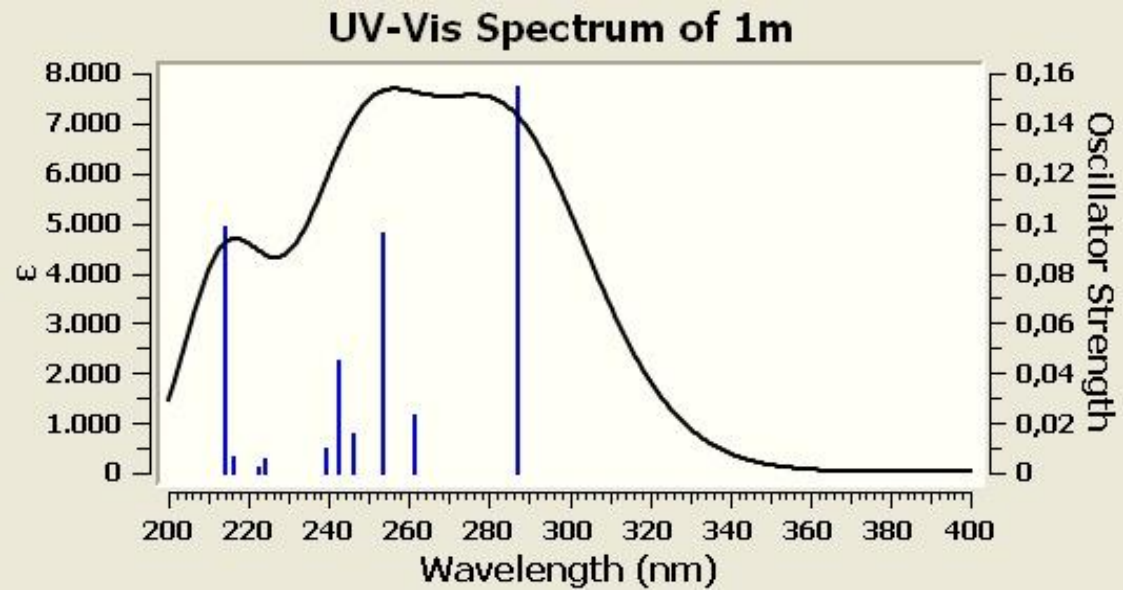


**Figure S20. UV-vis spectrum of gas phase of 1m at the ωB97XD/aug-cc-pVDZ level of theory.**

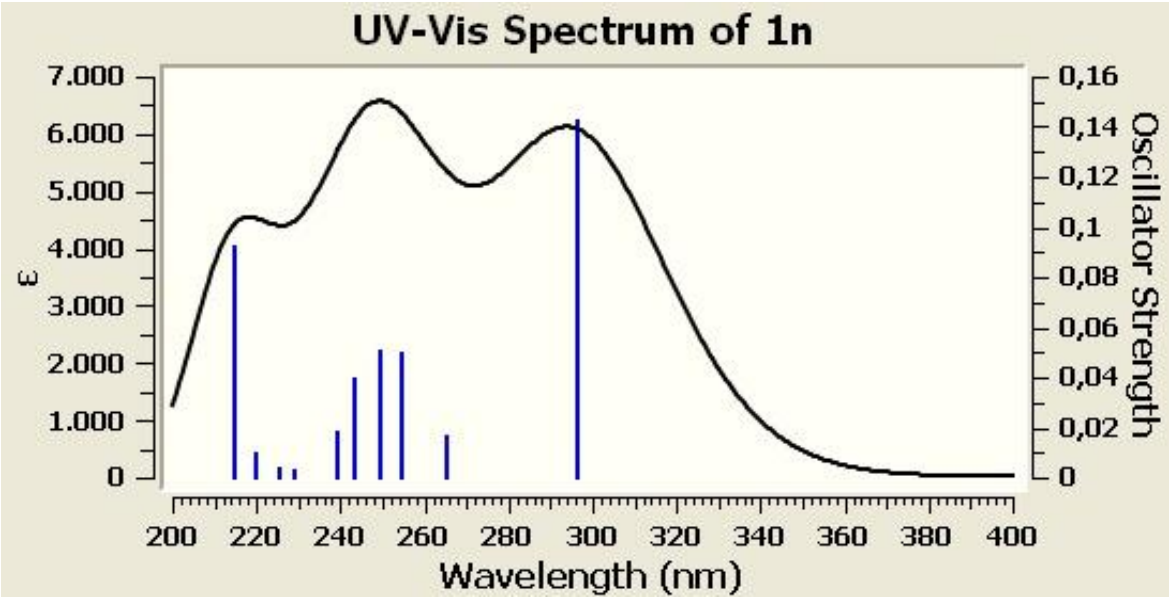


**Figure S21. UV-vis spectrum of gas phase of 1n at the ωB97XD/aug-cc-pVDZ level of theory.**

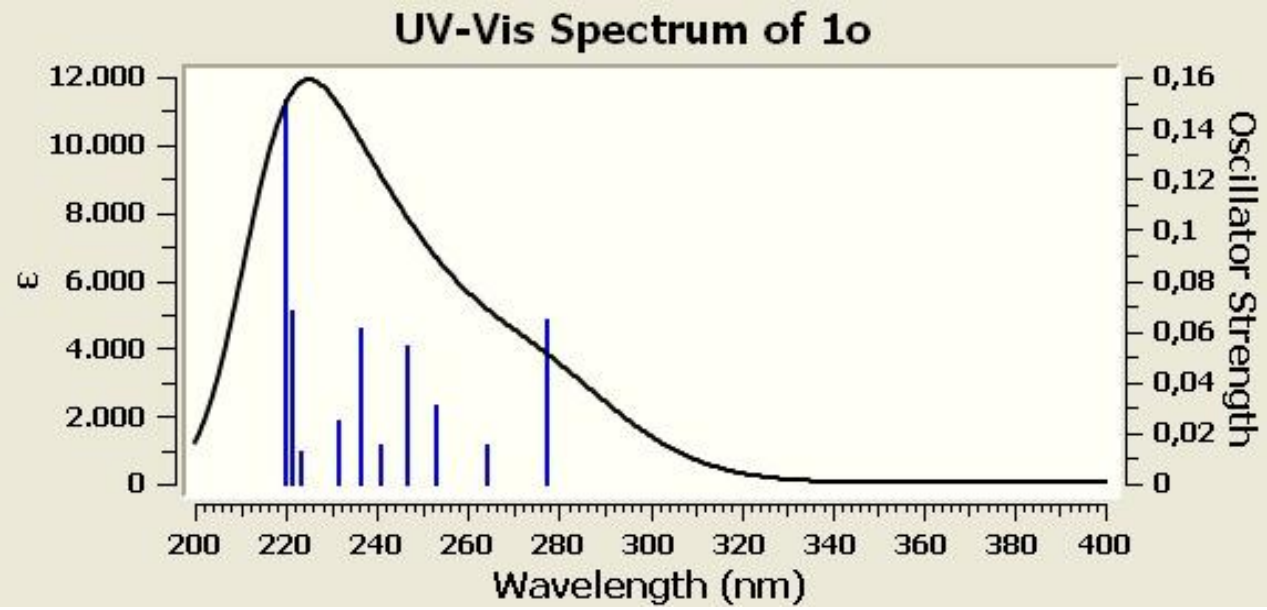


**Figure S22. UV-vis spectrum of gas phase of 1o at the ωB97XD/aug-cc-pVDZ level of theory.**

## References

[1] A. Austin, G. Petersson, M. J. Frisch, F. J. Dobek, G. Scalmani, and K. Throssell, "A density functional with spherical atom dispersion terms," J. Chem. Theory and Comput. 8 (2012) 4989. DOI: 10.1021/ct300778e

[2] J.-D. Chai and M. Head-Gordon, "Long-range corrected hybrid density functionals with damped atom-atom dispersion corrections," Phys. Chem. Chem. Phys., 10 (2008) 6615-20. DOI: 10.1039/B810189B
[3] J. M. Tao, J. P. Perdew, V. N. Staroverov, and G. E. Scuseria, "Climbing the density functional ladder: Nonempirical meta-generalized gradient approximation designed for molecules and solids," Phys. Rev. Lett., 91 (2003) 146401. DOI: 10.1103/PhysRevLett.91.146401
[4] V. N. Staroverov, G. E. Scuseria, J. Tao and J. P. Perdew, "Comparative assessment of a new nonempirical density functional: Molecules and hydrogen-bonded complexes," J. Chem. Phys., 2003, 119, 12129; [Erratum] 2004, 121, 11507(E)
[5] Guido, C. A.; Jacquemin, D.; Adamo, C.; Mennucci, B. Electronic Excitations in Solution: The Interplay between State Specific Approaches and a Time-Dependent Density Functional Theory Description. J. Chem. Theory Comput. 2015, 11, 5782–5790.
[6] Improta, R. The Excited States of π-Stacked 9-Methyladenine Oligomers: A TD-DFT Study in Aqueous Solution. Phys. Chem. Chem. Phys. 2008, 10, 2656–2664.
[7] Jacquemin, D.; Mennucci, B.; Adamo, C. Excited-State Calculations With TD-DFT: From Benchmarks to Simulations in Complex Environments. Phys. Chem. Chem. Phys. 2011, 13, 16987–16998.
[8] Mennucci, B.; Cappelli, C.; Guido, C. A.; Cammi, R.; Tomasi, J. Structures and Properties of Electronically Excited Chromophores in Solution from the Polarizable Continuum Model Coupled to the Time-Dependent Density Functional Theory. J. Phys. Chem. A 2009, 113, 3009–3020.
[9] Pedone, A. Role of Solvent on Charge Transfer in 7-Aminocoumarin Dyes: New Hints from TD-CAM-B3LYP and State Specific PCM Calculations. J. Chem. Theory Comput. 2013, 9, 4087–4096.
[10] Caricato, M.; Mennucci, B.; Tomasi, J.; Ingrosso, F.; Cammi, R.; Corni, S.; Scalmani, G. Formation and Relaxation of Excited States in Solution: A New Time Dependent Polarizable Continuum Model Based on Time Dependent Density Functional Theory. J. Chem. Phys. 2006, 124, 124520.
[11] Gaussian 16, Revision B.01, M. J. Frisch, G. W. Trucks, H. B. Schlegel, G. E. Scuseria, M. A. Robb, J. R. Cheeseman, G. Scalmani, V. Barone, G. A. Petersson, H. Nakatsuji, X. Li, M. Caricato, A. V. Marenich, J.

Bloino, B. G. Janesko, R. Gomperts, B. Mennucci, H. P. Hratchian, J. V. Ortiz, A. F. Izmaylov, J. L. Sonnenberg, D. Williams-Young, F. Ding, F. Lipparini, F. Egidi, J. Goings, B. Peng, A. Petrone, T. Henderson, D. Ranasinghe, V. G. Zakrzewski, J. Gao, N. Rega, G. Zheng, W. Liang, M. Hada, M. Ehara, K. Toyota, R. Fukuda, J. Hasegawa, M. Ishida, T. Nakajima, Y. Honda, O. Kitao, H. Nakai, T. Vreven, K. Throssell, J. A. Montgomery, Jr., J. E. Peralta, F. Ogliaro, M. J. Bearpark, J. J. Heyd, E. N. Brothers, K. N. Kudin, V. N. Staroverov, T. A. Keith, R. Kobayashi, J. Normand, K. Raghavachari, A. P. Rendell, J. C. Burant, S. S. Iyengar, J. Tomasi, M. Cossi, J. M. Millam, M. Klene, C. Adamo, R. Cammi, J. W. Ochterski, R. L. Martin, K. Morokuma, O. Farkas, J. B. Foresman, and D. J. Fox, Gaussian, Inc., Wallingford CT, 2016.

[12] Werner, H.-J.; Knowles, P. J. A second order multiconfiguration SCF procedure with optimum convergence. J. Chem. Phys. 1985, 82, 5053–5063.

[13] Knowles, P. J.; Werner, H.-J. An efficient second-order MC SCF method for long configuration expansions. Chem. Phys. Lett. 1985, 115, 259–267.

[14] Celani, P.; Werner, H.-J. Multireference perturbation theory for large restricted and selected active space reference wave functions. J. Chem. Phys. 2000, 112, 5546–5557.

[15] MOLPRO, version 2015.1, a package of ab initio programs, H.-J. Werner, P. J. Knowles, G.Knizia, F. R. Manby, M. Schütz, and others , see http://www.molpro.net.

[16] Dunning, T. H., Jr Gaussian Basis Sets for Use in Correlated Molecular Calculations. I. The Atoms Boron Through Neon and Hydrogen. J. Chem. Phys. 1989, 90, 1007−1023.